Small-Particle Research: Physicochemical Properties of Extremely Small Colloidal Metal and Semiconductor Particles

ARNIM HENGLEIN

Hahn-Meitner-Institut Berlin GmbH, Bereich Strahlenchemie, 1000 Berlin 39, FRG

Received March 8, 1989 (Revised Manuscript Received July 12, 1989)

Contents

Arnim Henglein was born in 1926 in Köln. He received his Dr. rer.nat. degree from the University of Mainz in 1951 and was a research associate at the Max-Planck-Institut für Chemie until 1953. He then joined Farbenfabriken Bayer in Wuppertal-Elberfeld where he worked until 1955. In 1956 he became a Privatdozent for Physical Chemistry at the University of Köln. From 1958 to 1960 he was a Visiting Fellow at the Mellon Institute, Pittsburgh, PA. He became full professor at the Technical University of Berlin and Director of the Section Strahlenchemie at the Hahn-Meitner-Institut Berlin in 1960. He was a visiting professor at the Universities of Kyoto, Florida (Gainesville, FL), Paris-Sud (Orsay), and Notre Dame (Notre Dame, IN) as well as at the Ecole Polytechnic Lausanne. His former research interests were in mass spectrometry, chemical dynamics, and phosphorus chemistry. Presently he is engaged in studies on the photochemistry, radiation chemistry, and electrochemistry of extremely small particles. He is also working on the chemical effects of ultrasound. In 1978, he was awarded the J. J. Weiss medal of the Association for Radiation Research (England) and, in 1988, the golden J. Heyrovský medal of the Academy of Sciences in Prague.

I. Introduction

During the past decade, "small-particle" research has become quite popular in various fields of chemistry and physics. By "small particles" are meant clusters of atoms or molecules of metals and semiconductors, ranging in size from <1 nm to almost 10 nm or having agglomeration numbers from <10 up to a few hundred, i.e., species representing the neglected dimension between single atoms or molecules and bulk materials.

Typical examples of small-particle research may be listed as follows (without attempting a complete literature review):[1] (1) synthesis of metal clusters in inorganic chemistry; (2) matrix isolation spectroscopy of clusters in noble gas matrices at low temperature; (3) molecular beam studies of clusters in vacuo; (4) metal clusters on supports in catalysis; (5) investigation of nanocrystalline materials;[2] (6) investigation of colloidal metal and semiconductor particles in solution or in the solid state after removal of the solvent.

The last example is the topic of the present article. Although colloid science developed many decades ago, little was known about extremely small colloidal particles (often called subcolloidal, not detectable in the ultramicroscope), despite the fact that such particles were often used as seeds for the growth of large ones. Some 10 years ago, systematic research on such particles was essentially initiated in the laboratory of the author in Berlin[3a–d] and in Prof. Grätzel's laboratory in Lausanne,[3e,f] and this research has since then spread to many other places. The reason for using colloidal metal and semiconductor solutions was to apply these materials as catalysts for free radical reactions initiated by light or ionizing radiation. In these reactions, electrons are transferred across the particle–solution interface similar to electrode reactions in electrochemistry. The small particles are therefore often referred to as "microelectrodes". Before the use of colloidal particles, Prof. Bard at the University of Texas, Austin, had already been successful in using TiO_2 powder suspended in water as a photosensitizer and catalyst.[4] A description of the mechanism of colloidal microelectrode reactions has been given in a recent review article.[3d]

It soon became evident during the photocatalysis studies that the small particles had certain physicochemical properties that made the investigation of the small particles per se an interesting new field of research. The "size quantization effects", already reviewed in ref 3d, constitute one aspect of this kind of research: the band structure in metals and semiconductors is not an atomic or molecular property but is brought about through the periodic arrangement of a

0009-2665/89/0789-1861$06.50/0

large number of atoms in a crystal lattice. A valid question is how many atoms are necessary to produce a valence and conduction band. In fact, many recent studies have shown that there exists a gradual transition from semiconductor or metal properties to molecular properties as the size of a crystal is successively decreased in the nanometer range. In this transition region, the optical and photocatalytic properties of semiconductors drastically change, and in the case of metals interesting changes in their electrochemical behavior are observed. Another aspect is the interactions of the charge carriers among themselves, which can be generated by light absorption in semiconductor particles at high local concentrations. These interactions can result in efficient photoelectron emission.[5] Further, nonlinear optical effects are present with respect to both the optical absorption[5,6] and third-order susceptibility.[7] Finally, progress has been made in improving particle properties by surface modification[8] and by preparing "sandwich" structures in which a particle consists of two semiconductor components.[9] In such sandwich structures, efficient primary charge separation has been achieved. Low-temperature experiments on fluorescence and hole burning[10] in frozen sols, Raman scattering at high pressure,[11] and NMR measurements[12] have also yielded important information on the properties of small particles. As size quantization effects have been reviewed quite recently,[3d] only the more recent developments are discussed in the present article.

Small-particle research of this kind is a new interdisciplinary branch of colloid science where photochemical, radiation chemical, and electrochemical methods and theories are applied. I would like to emphasize particularly the application of the methods of flash photolysis and pulse radiolysis in these studies. As described in more detail[3d] these methods allow one to investigate fast processes in and on the surface of colloidal particles. Both methods complement each other. For example, free radicals generated in the aqueous solvent by a short pulse of high-energy radiation diffuse to the colloidal particles and transfer an electron or inject a positive hole onto them. The fate of these charge carriers and the accompanying physical and chemical changes in the semiconductor particle can then be studied without being troubled by fast recombination with a carrier of opposite charge sign as in photochemical experiments.

II. Metals

A. Catalysis of Free Radical Reactions

The catalysis of radical reactions by colloidal metals has recently been reviewed[3d] and, for this reason, I will limit myself to just a few special topics. In all these studies, the colloidal particles were large enough (>1 nm) to have the properties of a metal. In the cases of silver and gold, the metal property is readily recognized by the presence of a band (Ag, 380 nm; Au, 520 nm) in the absorption spectrum which is caused by surface plasmon absorption of the electron gas. The idea in catalysis consists in producing free radicals in a colloidal solution by illumination or γ-irradiation which diffuse to the colloidal particles and transfer an electron to them. One colloidal particle may pick up a large number of electrons which are subsequently used to reduce substrates. The Fermi level in the metal is shifted to a more negative potential by electron pickup from the radicals; i.e., small particles act like an electrode on negative potential. Depending on the nature of the metal, there exists a certain overpotential for the production of hydrogen from the aqueous solvent. In the case of a metal of modest overpotential, such as silver, the particles can obtain a stationary negative potential increase as large as 1 V during hydrogen production.[13]

TABLE I. Relative Rate Constants for Multi-Electron-Transfer Reactions on the Silver Microelectrode[a]

reaction	rel rate constant
$2e^- + 2H_2O \rightarrow H_2 + 2OH^-$	1.0
$2e^- + CH_2Cl_2 + H_2O \rightarrow Cl^- + CH_3Cl + OH^-$	4.3×10^3
$2e^- + N_2O + H_2O \rightarrow N_2 + 2OH^-$	$>10^5$
$2e^- + Cd^{2+} \rightarrow Cd^0$	1.1×10^5
$8e^- + NO_3^- + 6H_2O \rightarrow NH_3 + 9OH^-$	1.1×10^6
$e^- + Tl^+ \rightarrow Tl^0$	$>10^6$
$e^- + Ag^+ \rightarrow Ag^0$	$>10^6$

[a] Relative rate constant = $[H_2O]/[S]_{1/2}$ is the concentration of substrate where the yield of H_2 from the reference reaction is decreased by 50%.

In systems of this type, the metal particles catalyze radical reactions which are highly exoergic but cannot occur in homogeneous solution because of a large negative activation entropy. For example, when CO_2^- radicals are generated in a silver sol, the following reactions take place:

$$Ag_n^{x-} + 2CO_2^- \rightarrow Ag_n^{(x+2)-} + 2CO_2 \quad (1)$$

$$Ag_n^{(x+2)-} + 2H_2O \rightarrow Ag_n^{x-} + H_2 + 2OH^- \quad (2)$$

and the overall reaction is

$$2CO_2^- + 2H_2O \rightarrow 2CO_2 + H_2 + 2OH^- \quad (3)$$

(Ag_n^{x-} is the silver particle of agglomeration number n which has already picked up x electrons); i.e., the metal particles catalyze the reduction of water by CO_2^- radicals.

Radical reactions in which more than one electron is to be transferred become possible as the electrons are stored on the catalyst and can subsequently be transferred to the substrate pairwise.[14] A number of multi-electron-transfer reactions on the colloidal silver microelectrode are listed in Table I. In these experiments, $(CH_3)_2COH$ radicals were generated in the silver sol, which charged the colloidal particles; the stored electrons partly produced H_2 from water and partly reduced the dissolved substrate. The relative rates given in the table were obtained by setting the rate of reaction 2 equal to 1 and calculating the rates from the half-concentration of the substrate where H_2 production was decreased by 50%. Some of the substrates are reduced at the mercury drop electrode in polarography at high negative overpotentials. However, at the charged colloidal silver particles they can be reduced with high rates at much lower potentials.

B. The Growing Microelectrode

Extremely small clusters of silver are generally not long-lived in aqueous solution at ambient temperature. The method of the growing silver microelectrode was used to study clusters during their growth in millise-

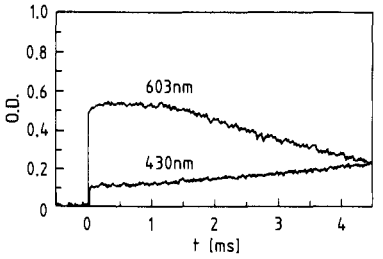

Figure 1. Growing silver microelectrode experiment. Absorptions at 603 and 430 nm as functions of time: 603 nm, decay of SPV^-; 403 nm, absorbance of both SPV^- and Ag_n.[17]

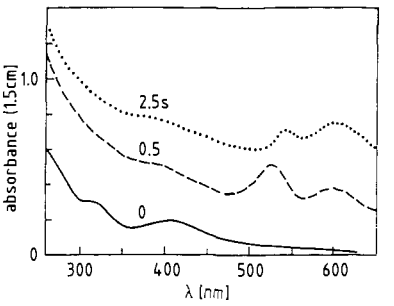

Figure 2. Absorption spectrum of nonmetallic gold particles (0) formed by a pulse of high-energy radiation and development of the spectra of larger metallic particles after 0.5 and 2.5 s.[18]

conds.[15] A solution containing a few 10^{-4} M Ag^+ ions was exposed to a short pulse of radiation producing a known amount of hydrated electrons in the 10^{-6} M range. The latter rapidly react with silver ions to form atoms, $Ag^+ + e_{aq}^- \rightarrow Ag^0$, which subsequently agglomerate to larger particles. These agglomerations were followed by recording the accompanying changes in optical absorption. At a certain particle size, i.e., after a certain time of agglomeration, metallic silver colloid was present, recognizable by the appearance of the 380-nm plasmon absorption mentioned above. The redox potential of the microelectrode

$$Ag_n \rightleftarrows Ag_{n-1} + Ag^+ + e^- \qquad (4)$$

becomes more positive as the particles grow. For n = 1 (free silver atom) the potential is −1.8 V[16] and, finally, for $n \rightarrow \infty$ the potential of 0.799 V of the conventional silver electrode is approached. The principle of the growing microelectrode consists in initiating a redox reaction at a certain point of growth, i.e., when the potential of the microelectrode, eq 4, has reached the appropriate value.

Two investigations of this kind have been reported. In the first case,[16] not only Ag atoms were produced by a pulse of radiation but also a known amount of Cu^+ ions (experimentally, this is achieved by using a solution containing both Ag^+ and Cu^{2+} ions; the hydrated electrons generated react in part with Ag^+ to produce Ag atoms and in part with Cu^{2+} to yield Cu^+). As long as the growing particles have an agglomeration number smaller than a critical number, n_{crit}, the Cu^+ ions do not react according to

$$Cu^+ + Ag^+ + Ag_n \rightarrow Cu^{2+} + Ag_{n+1} \qquad (5)$$

as the potential of the Ag^+/Ag_n system is still more negative than that of the Cu^{2+}/Cu^+ system, the latter being 0.2 V. However, when n exceeds n_{crit}, reaction takes place. Note that in this reaction additional silver atoms are formed, which can be recognized by the corresponding increase in the 380-nm absorption. It was found that the critical value of n for the occurrence of reaction 5 is 10; i.e., at this agglomeration number the potential of the microelectrode is close to 0.2 V. Details of these reactions have been reviewed recently.[3d]

In the second reaction, which has most recently been studied by Belloni and co-workers,[17] sulfonatopropylviologen (SPV) was used instead of Cu^{2+}. The pulse of radiation produces known amounts of the radical anion SPV^- and of Ag^0 atoms. SPV^- can readily be traced by its strong 603-nm absorption. During the initial stages of growth of the silver particles, reaction

$$SPV^- + Ag^+ + Ag_n \rightarrow SPV + Ag_{n+1} \qquad (6)$$

does not take place. However, when n = 5 is passed, reaction occurs. Figure 1 shows the temporal changes in the 603- and 430-nm absorptions of the pulsed solution. Immediately after the pulse, both absorptions are present. They belong to SPV^-, as the Ag^0 atoms do not absorb here. For about 1 ms the two absorptions do not change as during this time reaction 6 cannot take place. After this time, the silver particles have become large enough for reaction 6 to occur. The SPV^- signal at 603 nm decreases while that at 430 nm increases, the latter effect being due to the fact that the larger silver particles formed absorb here more strongly than SPV^-. Reaction 6 takes place at n_{crit} = 5, i.e., at a particle size substantially smaller than for reaction 5, as the redox potential of the SPV/SPV^- system (−0.41 V) is more negative than that of the Cu^{2+}/Cu^+ system. Experiments with the growing silver electrode are also of interest for the interpretation of the mechanism of the photographic plate development process where silver clusters start to act as centers for the reduction of additional silver ion when their size exceeds a critical value.

Experiments have also been carried out on the growing gold microelectrode.[18] The solution contained 1.7 × 10^{-4} M $NaAu(CN)_2$ and was exposed for 0.5 s to high-energy electrons. Under these circumstances all the gold complexes were reduced by hydrated electrons to yield gold atoms, $e_{aq}^- + Au(CN)_2^- \rightarrow Au^0 + 2CN^-$. The spectrum immediately after the irradiation (Figure 2) showed an unstructured UV absorption, the 520-nm band of metallic gold having not yet been developed. The spectrum therefore was attributed to nonmetallic gold species. However, after 1 s of growth the plasmon band at 520 nm was present, and after 2.5 s this band was red-shifted and a second band at much longer wavelengths appeared, indicating that finally rather large metallic gold particles were produced.

Potentials of microelectrodes for very small values of n can be calculated if the free energies of formation of the clusters involved are known. In a few cases, these data have been determined in experiments on metal vapor containing the dimer, trimer, etc. in equilibrium with the metal atoms.[19] When these data are used for calculating exact potentials in aqueous solutions they have to be corrected for the free hydration energies of the species involved. However, neglect of the latter does not lead to a great error as the free hydration energies of neutral inorganic species in water generally do not exceed 0.1 eV. The potential of silver electrodes as a function of n has been described previously.[3d] Figure 3 shows the results of a similar calculation for lead particles, knowing the thermodynamic data of the oli-

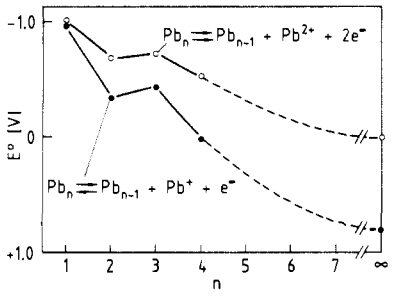

Figure 3. Standard potentials of the lead microelectrode as functions of agglomeration number n.

TABLE II. Rate Constants of Reactions of Ag^0, Ag_2^+, and $Ag_2^+ + NH_3$[a]

substance	rate constant [$M^{-1}s^{-1}$]		
	Ag^0	Ag_2^+	$Ag_2^+(NH_3)$
Fe^{3+}	1.2×10^9	3.0×10^8	
Cu^{2+}	6.5×10^8	$<10^5$	
O_2	5.0×10^9	4.6×10^8	7.0×10^9
H_2O_2	3.5×10^9	8.0×10^6	1.0×10^9
$CHBr_3$	3.0×10^9	5.0×10^8	2.0×10^9
$CHCl_3$	1.1×10^9	$<2 \times 10^5$	2.0×10^8
CCl_4	1.1×10^9	1.5×10^7	1.0×10^8
$ClCH_2COOH$	1.5×10^8	$<1.0 \times 10^6$	3.0×10^6
CH_3NO_2	2.3×10^9	1.1×10^8	1.5×10^8
$C_6H_5NO_2$	2.8×10^9	3.0×10^8	9.0×10^8

[a] Ammonia was present at 0.1 M.

gomeric molecules up to $n = 4$.[19] The conventional lead electrode has a potential of −0.126 V. The microelectrode

$$Pb_n \rightleftarrows Pb_{n-1} + Pb^{2+} + 2e^- \quad (7)$$

has a potential of about −1.0 V for $n = 1$ and shifts rather gradually toward a more positive potential with increasing n. In the case of the silver microelectrode, an oscillatory behavior had been noted at small n values.[3d] Figure 3 also shows the curve for the microelectrode system

$$Pb_n \rightleftarrows Pb_{n-1} + Pb^+ + e^- \quad (8)$$

Pb^+ being a short-lived but well-known species (it can be generated via reduction of Pb^{2+} by hydrated electrons or reducing organic radicals[20]). A Pb^+ ion on the surface of a compact lead electrode behaves like an Ag^+ ion on silver, the potential being rather positive. For $n = 1$ in eq 8, the potential is again close to −1.0 V.

C. Reactions of Silver Atoms in Solution

Silver atoms produced in the reduction of silver ions by hydrated electrons can react with other solutes, and the specific rates of these reactions can be determined in pulse radiolysis experiments. Similarly, the reactions of Ag_2^+, formed in the reaction of Ag^0 with Ag^+, with solutes can be investigated. In all these reactions, the silver species act as strong electron donors. Reactions and their rate constants are listed in Table II. It can be seen that Ag^0 reacts faster than Ag_2^+ and that the reactions of the latter are accelerated in the presence of ammonia. These effects are understood in terms of the more negative redox potential of the uncomplexed silver atoms, the standard potential $E°(Ag^+/Ag^0)$ being −1.8 V, and $E°(2Ag/Ag_2^+) = -1.2$ V. In the presence of ammonia these potentials shift to more negative

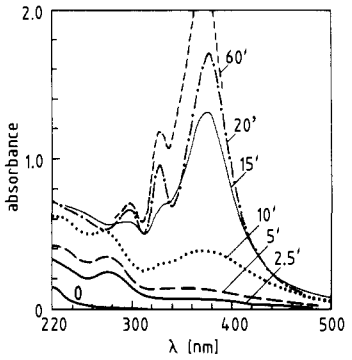

Figure 4. Absorption spectra of a silver salt solution containing polyphosphate during radiolytic reduction at various times of γ-irradiation.[22]

values; for example, $E°(Ag(NH_3)_2^+/Ag^0 + 2NH_3) = -2.2$ V.[21]

D. Long-Lived Silver Clusters in Solution

As already pointed out, metal clusters are generally short-lived in aqueous solution as they rapidly agglomerate. However, if the intermediate clusters could be stabilized, one could investigate their properties and observe their chemical reactions. Such a stabilization has recently been achieved in the case of silver clusters formed in the radiolytic reduction of Ag^+ ions in the presence of sodium polyphosphate.[22] The latter is known to be an excellent stabilizer for many inorganic colloids. In this experiment, a solution containing 2×10^{-4} M Ag^+ ions, 2×10^{-4} M polyphosphate, and 0.1 M 2-propanol was γ-irradiated. Under these conditions, reducing radicals, i.e., hydrated electrons and 1-hydroxymethylethyl radicals, were generated which reduce silver ions. The absorption spectrum of the solution before and after various times of irradiation is shown in Figure 4. In the beginning of the reduction, a band appears at 275 nm, and with increasing conversion this band becomes stronger and the 380-nm plasmon band of silver starts to develop. At longer times, the 275-nm band disappears, new bands at 300 and 325 nm develop, and simultaneously the 380-nm band becomes much stronger.

The absorptions at 275, 300, and 325 nm were attributed to nonmetallic silver clusters stabilized by polyphosphate. It was not yet possible to assign cluster structures to the various maxima observed, although the spectra of silver clusters in rare gas matrices are known.[1b] In fact, one cannot expect a clear correlation between the spectra in aqueous solution and matrices. For example, the silver atom has its maximum at 360 nm in water,[21] while it absorbs at substantially shorter wavelengths in an argon (292–310 nm) and a xenon (322–333 nm) environment.[1b] The lifetime of the clusters in the absence of air was several hours. The clusters have strong reducing power. Their absorption disappears immediately upon exposing the irradiated solution to air. They also react with carbon tetrachloride, Cu^{2+} ions, and nitrobenzene. In the latter two reactions, the absorptions of the clusters disappear and the 380-nm band of metallic silver is increased. Cu^{2+} and nitrobenzene act as catalysts for the conversion of the nonmetallic silver clusters to larger particles of metallic silver. The mechanism proposed contains the following elementary steps: (1) reaction of clusters (m

= small number) with Cu^{2+} ions or $C_6H_5NO_2$ because of the high negative potential of these clusters

$$Cu^{2+}(C_6H_5NO_2) + Ag_m \rightarrow Cu^{+}(C_6H_5NO_2^{-}) + Ag^{+} + Ag_{m-1} \quad (9)$$

followed by further reduction reactions of Ag_{m-1} with copper ions or nitrobenzene, and (2) reoxidation of the reduced species formed on larger metallic silver particles (n = larger number) in the solution which have a more positive potential

$$Cu^{+}(C_6H_5NO_2^{-}) + Ag_n \rightarrow Cu^{2+}(C_6H_5NO_2) + Ag_n^{-} \quad (10)$$

followed by the increase in size of the metallic particles:

$$Ag_n^{-} + Ag^{+} \rightarrow Ag_{n+1} \quad (11)$$

The silver clusters were found to be very sensitive to UV light. Their absorption bands rapidly disappear upon illumination of the solution and at the same time the 380-nm band increases. It thus seems that UV light also catalyzes the transformation of nonmetallic clusters to larger particles of colloidal silver. The mechanism proposed is similar to the above mechanism for catalysis by copper ions. The first step is the photoemission of an electron

$$Ag_m + h\nu \rightarrow Ag_{m-1} + Ag^{+} + e_{aq}^{-} \quad (12)$$

followed by the capture of the electron by a larger Ag_n particle

$$Ag_n + e_{aq}^{-} \rightarrow Ag_n^{-} \quad (13)$$

and reduction of Ag^{+} from reaction 12 on the Ag_n^{-} particle formed (eq 11).

E. Final Remarks

Conventional electrochemistry has developed the basic concepts of the redox chemistry of compact electrodes. During the past two decades, impulses from other fields of physical chemistry, such as photochemistry and radiation chemistry, have come to generate metal atoms in solution and study their redox behavior. The intermediate stage of metal cluster redox chemistry is still in its infancy, our present knowledge being rather fragmentary. The present article is to point out to the reader the existence of this field, in which many reactions occur in a direction opposite to that of conventional redox reactions on compact metal electrodes.

III. Semiconductors

A. Size Quantization Effects

The changes in the absorption spectrum of cadmium sulfide with changing particle size, as shown in Figure 5, illustrate the effect of size quantization. Particles larger than about 6 nm, i.e., larger than the size of an exciton in the macrocrystalline material, start to absorb close to 515 nm (or 2.4-eV photon energy, corresponding to the band gap of bulk CdS). With decreasing size, the absorption threshold shifts to shorter wavelengths. CdS consisting of particles below 2.2 nm is colorless. It can be recovered as a white powder from the aqueous solution where it was formed by precipitating Cd^{2+} ions with H_2S in the presence of a small amount of sodium polyphosphate (the solid powder obtained after removal of the solvent also contains the polyphosphate; it prevents the small particles from coming into close contact). Note also that the absorption spectrum of the smallest particles in Figure 5 is structured. In the case of semiconductors having a band gap smaller than that of CdS, the color changes are even more drastic. For example, cadmium phosphide, a black material with a band gap of 0.5 eV, can be made in all colors of visible light by decreasing the particle size between 10 and 2 nm.[23] The fluorescence band of the colloids is also blue-shifted with decreasing particle size. Color pictures of such quantized semiconductor materials ("Q" materials) have previously been published.[24]

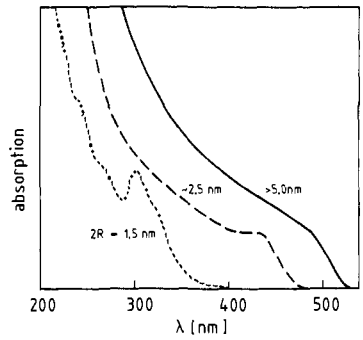

Figure 5. Absorption spectrum of CdS in aqueous solution: different mean particle sizes.

Light absorption leads to an electron in the conduction band and a positive hole in the valence band. In small particles they are confined to potential wells of small lateral dimension and about 3 eV deep (energy difference between the position of the conduction band and a free electron), and this leads to a quantization of their energy levels (which in the bulk material constitute virtual continua in the conduction and valence bands). The phenomena arise when the size of a colloidal particle becomes comparable to the de Broglie wavelength of a charge carrier. The effective mass of an electron in a crystal lattice often is substantially smaller than that of an electron in free space; i.e., the de Broglie wavelength is rather long and therefore the effects can already be seen in particles a few nanometers in diameter. The size quantization effects occur most drastically in low band gap materials where the effective mass of the electron is particularly small.

CdS, ZnO, and PbS are the materials where the shift of the absorption threshold with particle size has been studied in most detail. Figure 6 shows the wavelength of the absorption threshold (and band gap energy) as a function of particle size. The experimental data can be well explained by the current theories. As was first shown by Brus,[25] the electron and hole may be treated as particles in a spherical box with an infinitely high potential at the interface. The effective masses of the corresponding species were assumed to be the same as in the macrocrystalline material, and a correction was made for their Coulombic attraction. In later calculations, improvements have been made by using Hylleraas functions[26] and a finite potential well.[8c,27] A principal difficulty consists in using the effective mass of the bulk material as this is correct only when one is dealing with electronic states close to the edges of the band gaps.

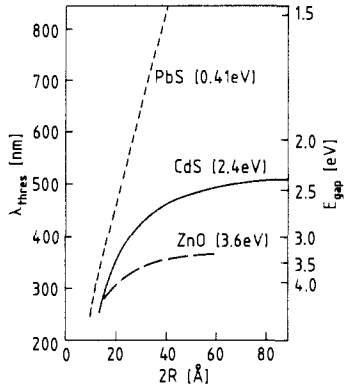

Figure 6. Wavelength of absorption threshold as a function of particle size for CdS,[8c] ZnO,[41] and PbS.[28] Right: band gap energy. The gap energies of the macrocrystalline materials are given in parentheses.

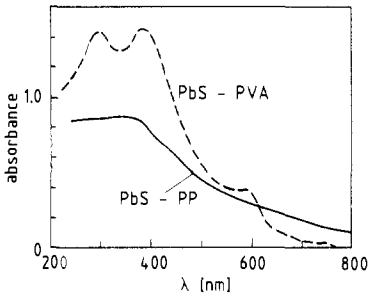

Figure 7. Spectrum of Q-PbS formed in the presence of polyphosphate (PP) and poly(vinyl alcohol) (PVA).

The effective mass is a collective property of a crystal. As the crystal contains fewer and fewer atoms, the collective properties should become less pronounced; i.e., the effective mass increases with decreasing particle size. In fact, a recent study on PbS has shown that the effective mass approximation becomes incorrect already at rather large particle sizes, and a hyperbolic band model was proposed.[28]

Size quantization effects are observed today in many systems. A few applications in the preparation of colloidal sandwich structures are described below. Unusual observations have been made in thermal and ultrasonic dissolution experiments: When a powder of MoS_2 or WS_2 is heated at 60 °C in acetonitrile for 3 days, a colloidal solution is obtained that contains 1.0–3.5-nm particles whose spectrum is strongly blue-shifted with respect to that of the macrocrystalline material.[29] Similarly, powders of MoS_2 and WSe_2 suspended in water can be partly brought into solution by intense ultrasonic treatment.[30] These solutions are transparent after filtration and contain quantized particles of about 3 nm. The chalcogenides of molybdenum and tungsten have a layered structure with strong ionic bonds within and weak van der Waals forces between the layers. The van der Waals layers can readily be cleaved by penetrating solvent molecules or by the hydrodynamic shear forces existing in a solution in which cavitation is produced by ultrasound.

Stabilizing polymers are often used in the preparation of colloidal solutions. Very little is known about the interaction between the colloidal particles and the polymers. This interaction can influence the kinetics of particle growth, i.e., the final shape and size distribution of the particles. A typical example is shown in Figure 7, where one finds absorption spectra of Q-PbS.[31]

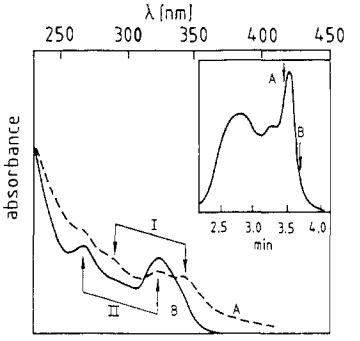

Figure 8. Absorption spectra of two fractions (A and B) obtained in the chromatography of colloidal CdS. Inset: Chromatogram of the CdS solution.[32b]

Macrocrystalline lead sulfide has a band gap of only 0.41 eV and begins to absorb in the infrared. The solutions in Figure 7 contain either sodium polyphosphate or poly(vinyl alcohol) as stabilizer. In both cases quantized particles are formed as the onset of absorption lies in the visible. However, in the case of polyphosphate the spectrum of PbS is not structured, while a structure with a typical exciton maximum at 600 nm and two maxima at 300 and 400 nm exists in the case of the poly(vinyl alcohol) stabilizer. In the latter case, the PbS particles have a rather narrow site distribution. The bands at 300 and 400 nm are possibly due to oligomeric PbS particles.

B. The Question of "Magic" Agglomeration Numbers

The maxima that appear in the absorption spectrum of very small particles of CdS (Figure 5) and other materials can be brought about by two effects: (1) They correspond to optical transitions to various discrete energy levels in the quantized particles. (2) They correspond to the optical transition to the first excited state, which has the greatest oscillator strength, in quantized particles of different size; i.e., "magic" agglomeration numbers exist in the size distribution of the sample. Magic numbers can arise if certain sizes have particular stability or because of the kinetics of particle growth. The latter possibility is explained as follows: The colloids are generally made by a fast precipitation. After a short time, in the millisecond range, the precipitation is completed and a primary size distribution of extremely small particles is present, peaking at an agglomeration number n_{max}. If the particles subsequently grow to a certain extent via association, the originally most abundant agglomeration number n_{max} will be preserved in the final distribution in the form of integer multiples.

Spectrometric methods alone are not sufficient to unveil the origin of the absorption maxima in the spectrum of very small particles. Exclusion chromatographic methods have recently been developed to fractionate colloidal particles.[32] Figure 8 shows a typical example. The inset of the figure shows the chromatogram of a CdS solution. It was obtained by recording the 250-nm absorption of the solution behind the column, the absorption coefficient of CdS being independent of particle size at this wavelength. It can be seen that the sample had mainly two size distributions. In reading the chromatogram one should remember that smaller particles appear at longer elution times.

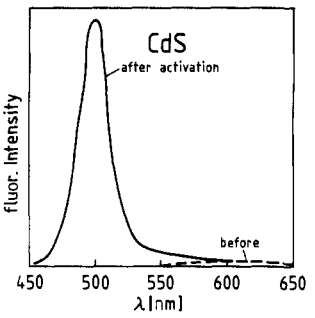

Figure 9. Fluorescence spectrum of CdS before and after surface modification.

The absorption spectra of the fractions A and B are shown in the main part of Figure 8. Spectrum A has four weak maxima. In going to B, two maxima (designated by I) disappear while the other two (designated by II) become stronger. This result was interpreted as two magic numbers being present in the size range of fractions A and B, particles of each magic number producing two absorption maxima that correspond to the transitions to the first and second excited states in these particles.[32b]

C. Surface Modification

A large percentage of the atoms in a nanometer particle are on the surface, where dangling bonds, adsorbed species, etc. produce traps for electrons and holes. The fate of the charge carriers generated by light absorption is strongly dependent on the existence of these traps. Fluorescence experiments are suitable to demonstrate this fact. Figure 9 illustrates a drastic example. The fluorescence spectrum of a CdS sample is shown here before and after surface modification. CdS colloids made by adding H_2S to a cadmium salt solution have generally a very weak red fluorescence, peaking at a photon energy about 0.4 eV below the absorption threshold. This fluorescence is explained as radiative recombination of trapped charge carriers, the competing radiationless recombination being the dominant process. After surface modification by the addition of 300% Cd^{2+} ions and an increase in pH to 11, a bright green-blue fluorescence is present, the quantum yield exceeding 50%. The maximum of this fluorescence lies at the absorption threshold; i.e., one is dealing with band gap recombination of the free charge carriers.

The effect was explained by the formation of a layer of cadmium hydroxide, where Cd^{2+} ions are coordinatively bound to surface sulfide anions to form (S^{2-} $Cd^{2+}OH^-$) structures, which block the surface imperfections responsible for the trapping of charge carriers. The CdS particles in Figure 9 had a mean diameter of 6 nm before surface modification, and they became substantially larger by the cadmium hydroxide layer as could be seen in dynamic light scattering experiments. The stability of the particles toward both light and OH radical attack was also quite significantly increased by several orders of magnitude.[8c]

Colloidal particles may be made soluble in organic solvents by appropriate surface derivatization. Two approaches have been reported. Steigerwald et al. treated a cadmium selenide colloid, which had been made in inverse micelles, with phenyl(trimethylsilyl)-selenium. A solid material precipitated which consisted

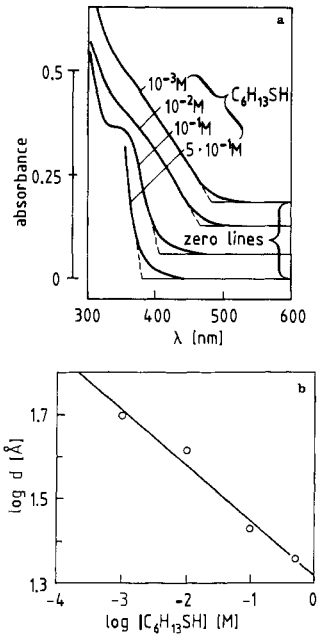

Figure 10. (a) Onset of absorption of CdS samples prepared in tetrahydrofuran solution in the presence of various concentrations of $C_6H_{13}SH$ (CdS concentration: 2×10^{-4} M). (b) Long-chain derivatization of CdS particles: mean diameter as a function of thiol concentration during particle growth.[34b]

of CdSe crystallites covered covalently with phenyl ligands. It could be redissolved in pyridine.[33] Nosaka et al.[34a] observed that CH_3S groups were built onto the surface when CdS was precipitated in aqueous solution in the presence of sodium methylthiolate. Fischer et al.[34b] prepared CdS by adding H_2S to a solution of cadmium salt in tetrahydrofuran containing various long-chain alkanethiols. The solvent and excess alkanethiol were removed by distillation, and a cadmium sulfide powder or oil remained that was soluble in many organic solvents. Depending on the concentration of alkanethiol, quantized particles of different absorption and fluorescence color were formed. Figure 10a shows the beginning of the absorption spectrum of CdS prepared in the presence of different amounts of thiol, and Figure 10b gives the relation between mean particle diameter and thiol concentration. The thiol is regarded to act as a terminator for the growth of the colloidal particles; it is solidly built into the surface of the particles. The thiols exert their action only when they are present during the precipitation procedure; addition of thiol to a CdS sol in tetrahydrofuran after preparation of the sol does not lead to surface derivatization.[34b]

Similar observations were made by Hayes et al.,[35] who prepared CdS colloids by a radiolytic procedure in aqueous solutions containing benzenethiol. They also obtained colloidal particles that were stabilized by phenyl groups on the surface.

D. Colloidal Sandwich Structures

In a colloidal sandwich structure two different semiconductor parts are connected. Illumination into one part may produce a response in the other part or at the interface between the two. The first example was found in experiments where small amounts of cadmium salt were added to a ZnS sol. As the solubility product of CdS is smaller than that of ZnS, Zn^{2+} ions are substituted by Cd^{2+} ions on the surface of the particles and

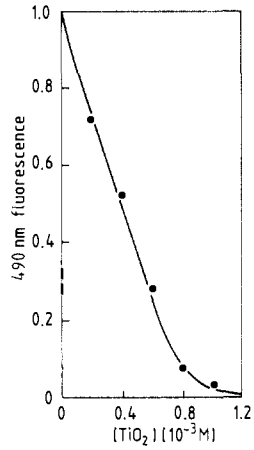

Figure 11. Fluorescence quantum yield of a CdS sol as a function of the concentration of added TiO_2.[9a]

a layer of approximate composition $CdZnS_2$ is formed. Just a few Cd^{2+} ions on a ZnS particle are sufficient to quench the fluorescence of the latter. At higher cadmium amounts the fluorescence of the 1:1 layer of zinc and cadmium sulfide appears upon illumination into the ZnS part of the sandwich. These findings show that the transfer of charge carriers from one part of the sandwich structure to the other is possible.[8a]

More recently, sandwich structures between cadmium sulfide as the light-absorbing semiconductor part having a relatively small band gap and titanium oxide or zinc oxide as the large band gap part have been described.[9] Such structures form spontaneously when the separately prepared solutions of the colloids are mixed under certain conditions where there is a large excess of Cd^{2+} in alkaline solution, polyphosphate acting as stabilizer. The formation of the sandwich is recognized by the quenching of the fluorescence of CdS. Figure 11 shows an example, where the fluorescence quantum yield is plotted versus the concentration of added TiO_2 sol. Practically complete quenching is observed. The effect was explained as immediate transfer of the electron formed in the illuminated CdS part of the TiO_2 part as the conduction band in TiO_2 is on a less negative potential than that of CdS. This mechanism is similar to charge-transfer quenching of an excited state as often occurs in organic photochemistry. The positive hole, on the other hand, cannot move to the TiO_2 part as it would be there on a much higher positive potential than in CdS. The result of this electron transfer is an efficient primary charge separation. The TiO_2–CdS sandwich thus acts as a small diode of almost molecular dimensions or like an n–p junction, although the mechanism of charge separation is different (as depletion layers in small colloidal particles, which in compact semiconductors produce useful potential gradients, are practically not operative, the size of the particles being much smaller than the dimension of several 10 nm of a depletion layer).

As a result of the efficient primary charge separation, certain chemical reactions induced by light absorption in the CdS part occur with much higher quantum yield than in the case of simple CdS catalyst particles.[9a] Figure 12 shows as an example the reduction of methylviologen, MV^{2+}, in CdS solutions containing different TiO_2 concentrations. The quantum yield for the formation of the radical cation, MV^+, which can readily

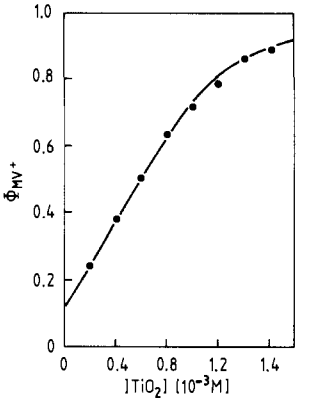

Figure 12. Quantum yield of methylviologen reduction in a CdS sol as a function of added TiO_2.

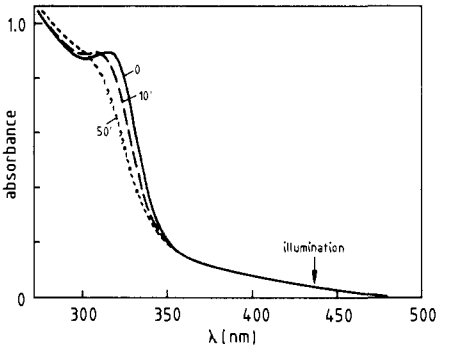

Figure 13. Absorption spectrum of a CdS–ZnO colloid before and after illumination with 430-nm light.[9a]

be detected by its strong blue color, is about 10% in the absence of TiO_2 and increases to almost 100% in its presence. Figure 13 shows a result obtained upon illumination into the CdS part of a CdS–ZnO structure. The absorption spectrum of the solution is shown before and after illumination. It can be seen that the absorption starts at 490 nm, which is due to CdS, and rises steeply at 350 nm, where ZnO starts to absorb. The response of the 430-nm illumination of the CdS part appears in the 320–350-nm range, where the absorption of the ZnO part is decreased. This proves that an electron had been transferred to the ZnO part as excess electrons on ZnO are known to shift the absorption threshold to shorter wavelengths (see below).

Similar effects have been found with sandwich structures of Cd_3P_2 and ZnO.[9b] As mentioned above, cadmium phosphide can be made with different band gaps by varying the particle size. Quenching of the fluorescence of cadmium phosphide by ZnO was more efficient the larger the band gap of the Cd_3P_2 part. Similarly, the response in the 320–350-nm absorption of ZnO became stronger with increasing band gap of Cd_3P_2. These findings were explained by the increasing driving force for electron transfer from the illuminated cadmium phosphide part to ZnO as the conduction band in Cd_3P_2 moves to more negative potential with decreasing particle size.

A phenomenon quite different from the ones just described was observed in the case of CdS–Ag_2S[36] and AgI–Ag_2S[37] structures. Such structures are formed upon the addition of silver ions to a CdS sol or H_2S to an AgI sol, respectively. In both cases a strong red fluorescence arises which moves into the infrared region with increasing size of the Ag_2S part. This can be seen

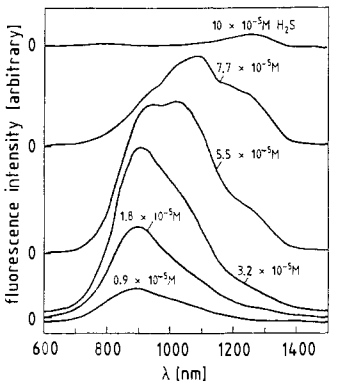

Figure 14. Fluorescence spectrum of a 2×10^{-4} M AgI sol after addition of various amounts of H_2S.[37]

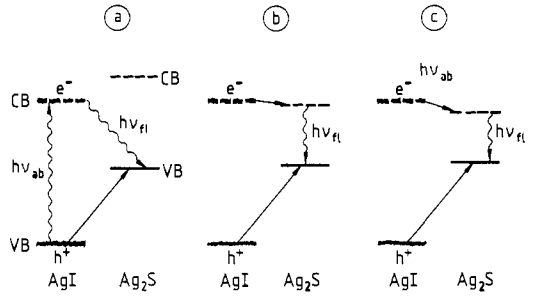

Figure 15. Term scheme in AgI–Ag_2S sandwich structures: (a) small, quantized Ag_2S part; (b) larger, but still quantized Ag_2S part; (c) large, nonquantized Ag_2S part. (VB, valence band; CB, conduction band; $h\nu_{fl}$, fluorescence light.[37]

from the fluorescence spectra in Figure 14, where different amounts of hydrogen sulfide were added to an AgI sol. AgI itself fluoresces at 450 nm. This fluorescence is quenched by a small amount of Ag_2S. The new red fluorescence peaks at 850 nm (1.45-eV photon energy) at low Ag_2S deposits. A second maximum at 1050 nm (1.18 eV) appears at higher Ag_2S concentrations, which shifts to longer wavelengths with increasing Ag_2S concentration, and, at almost complete conversion of AgI into Ag_2S, a weak fluorescence at 1250 nm (0.99 eV) remains that corresponds to the band gap energy of nonquantized Ag_2S.

The explanation of these findings is given by Figure 15, where the term scheme of three AgI–Ag_2S pairs is shown. Small silver sulfide deposits (a) are strongly quantized, the conduction band lying at more negative potential than that of AgI. The hole generated in illuminated AgI moves to the Ag_2S part at the interface, and the 850-nm emission is brought about by the recombination of the electron in the conduction band of AgI with this hole in Ag_2S. When the Ag_2S deposit is sufficiently large (b), its conduction band is at a less negative potential and the electron can also be transferred from AgI to Ag_2S. The recombination occurs now in the Ag_2S part, the emitted light having longer and longer wavelengths as the band gap of Ag_2S becomes smaller with increasing size of this part of the sandwich. It has also been pointed out that similar size quantization effects occur in the photographic plate when AgBr grains are activated by sulfur sensitization.[37]

E. Excess Electrons on Particles

In a compact n-type semiconductor of high doping level the absorption threshold is blue-shifted (Burstein–Moss effect[38]), which is explained by a band-filling

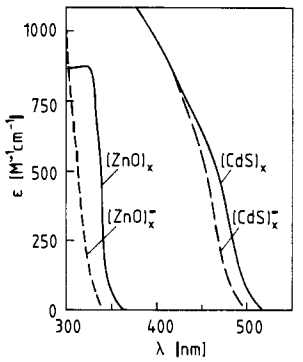

Figure 16. Absorption spectra of CdS and ZnO in aqueous solution before and after the addition of one excess electron per particle.

mechanism. The lower levels in the conduction band are occupied and light absorption can therefore begin only at higher photon energies at which electrons are promoted from the valence band into higher states of the conduction band. The shift becomes noticeable at an electron concentration where the average distance between the charge carriers is comparable to the size of an exciton in the material. Let us now consider an experiment in which a small part having the size of an exciton is cut out from the semiconductor sample. It will contain just on excess electron. Does the Burstein–Moss shift still occur?

This experiment was performed by using pulse radiolysis.[6] Hydrated electrons were generated in a colloidal CdS solution by a pulse of high-energy radiation. The hydrated electrons, which are readily recognized by their strong absorption at 700 nm, diffuse to the colloidal particles and react with them. When the course of this reaction was followed at a wavelength shortly below the absorption threshold of the CdS particles, an absorption decrease was observed due to the blue-shift of the absorption of the particles. The negative absorption coefficient (per hydrated electron generated) in the maximum bleaching at 475 nm was 5×10^4 M^{-1} cm^{-1}. On the other hand, CdS absorbs at this wavelength with only 400 M^{-1} cm^{-1} (per CdS molecule). Obviously, the electron deposited does not affect just one CdS molecule but a large number of molecules. In other words, the excess electron influences an optical transition at the absorption threshold where the wave function extends over practically the whole colloidal particle. Figure 16 shows the absorption spectrum of CdS before and after addition of one electron per particle.

It is not clear at present whether this blue-shift in a small particle is indeed explained by the band-filling mechanism. The electron deposited on the particle is probably not in a free state but localized in a shallow trap on the surface. Under these circumstances, the usual interpretation of band filling by conduction band electrons seems questionable. Other mechanisms have therefore been proposed such as the polarization of the exciton generated by light absorption in the electric field of the excess electron; this would lead to a size quantization effect, as the electron of the exciton is confined to less space in the particle.[6] Another explanation involves an interaction of the exciton with excess negative or positive charge carriers which reduces the oscillator strength of the exciton transition.[7b] On the other hand, Liu and Bard have recently reported cal-

culations that led them to the conclusion that even a fraction of an elementary negative charge donated into a CdS particle would lead to a noticeable shift of the absorption threshold.[39] Such a fraction of charge could be donated by a trapped electron or even by strongly adsorbed anions. In fact, it was reported by Kormann et al.[40] that the absorption threshold of small TiO_2 particles can be shifted reversibly to the blue or red by chemisorption of OH^- or H^+ ions, respectively. No attempt is made here to present a final interpretation of all these observed shifts but I would like to point out the problem to encourage further experiments in this direction.

The blue shift has also been studied for colloidal ZnO, where it is particularly strong. Figure 16 shows also the absorption spectrum of a ZnO sol before and after the deposition of one electron per particle. The electrons were donated by hydroxymethyl radicals, $\cdot CH_2OH$, generated radiolytically.

In these experiments, the electron was deposited from outside onto the colloidal particles. The question then arose whether the electrons that are generated within the particles by light absorption also cause the spectrum to shift. Upon illumination a stationary electron concentration is formed as electrons and holes are continuously produced and disappear by recombination. It was found that, under laser illumination, sufficient stationary electron concentration was produced to make the spectrum shift to shorter wavelengths. In the case of CdS the bleaching signal was found to follow the profile of a 30-ns laser pulse.[5b] On the other hand, in the case of ZnO, where bleaching is stronger, the signal is long-lived.[41] The blue shift in the illumination of small particles constitutes a nonlinear optical absorption effect.[6] One could imagine the construction of an optical switch on the basis of this effect. The bleaching effect has also been made responsible for the nonlinear optical effects observed in four-wave-mixing experiments with CdS particles embedded in a polymer matrix.[7b]

To complete the "excess-electron story", a few words are in order about what happens when more than one electron is stored on a colloidal particle. This has been studied in detail for CdS.[6] The second electron causes an additional blue shift of the spectrum. However, whereas one excess electron may live for minutes on a colloidal particle, two electrons react to yield a cadmium atom, and finally a metal deposit is formed upon further electron deposition.

F. Photoelectron Emission

Photoelectron emission from CdS and ZnS particles in aqueous solution was one of the first reactions discovered in laser flash photolysis of colloidal solutions.[5a] Immediately after the flash of a frequency-doubled ruby laser (λ = 347.2 nm; 3.57 eV) the absorption spectrum of the hydrated electron was recorded. In later studies,[5b] the absorption of the remaining hole was detected. The greatest quantum yield observed was 0.07 electron emitted per absorbed photon, which exceeds the yields encountered in photoemission experiments with compact semiconductor electrodes[42] by several orders of magnitude.

An electron can be emitted from a colloidal particle if the energy of the absorbed photon is larger than E_g + ΔE, where E_g is the band gap energy and ΔE the difference in the energies of the hydrated electron and the lower edge of the conduction band. E_g is 2.4 eV for CdS; the energy of e_{aq}^- is −2.9 eV on the standard electrochemical energy scale, and that of the conduction band in CdS is −0.6 to −0.9 eV depending on pH. Thus ΔE is 2.0–2.3 eV. The energy of the laser used (3.57 eV) is 0.7–1.0 eV below the expected threshold for electron emission. The fact that emission occurred was a first indication for the two-photon nature of the process.

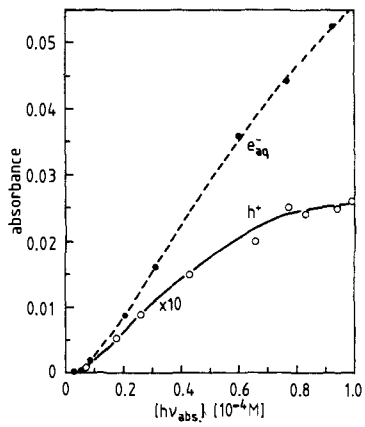

Figure 17. Laser photoelectron emission from CdS: absorption of emitted electrons and remaining holes as functions of the absorbed photon concentration.[5b]

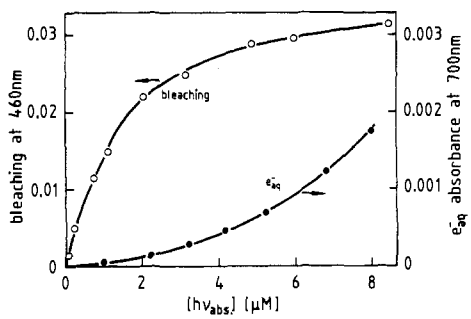

Figure 18. Photoelectron emission from CdS: 460-nm bleaching during the laser flash and absorption of emitted electrons as functions of the absorbed photon concentration.[5b]

Photoelectron emission was also observed for colloidal cadmium phosphide in aqueous solution.[5c] It seems that in all these emission processes the solvent has to be water. No emissions were observed in acetonitrile or alcohol solutions of CdS. It also seems that emission is limited to solutions that contain a polyanionic colloid stabilizer, such as colloidal silicon dioxide or polyphosphate. The electron is promoted by sequential absorption of two photons into a high-lying level in the conduction band of a particle, from where it can tunnel into the aqueous solvent. The negative charge of the stabilizer prevents the emitted electron from rapid return by electrostatic repulsion, which may be the reason for the process occurring only in the presence of a polyanion. Further, high yields are only observed when the particle size is small. Two reasons may be given for this: first, the tunneling distance into the aqueous solvent is short, and second, as the density of states in the conduction band is low, because of the quantization of the small particles, the rate of the competing thermalization of the electron within the particle decreases.

Figures 17 and 18 show typical results of photoelectron emission experiments on CdS. The absorptions

of the emitted electrons and remaining holes are plotted in Figure 17 as functions of the absorbed laser dose, the latter being expressed as concentration of absorbed photons. At low doses, the yields increase more rapidly than proportional to the dose, which is typical for a process in which two photons are involved. This can also be seen from Figure 18, where the low-dose part of the curve for e_{aq}^- is shown on a more expanded scale. At higher doses, the e_{aq}^- absorption increases faster than that of h^+. This effect is due to the fact that several electrons are emitted from a colloidal particle, the remaining holes reacting rapidly with each other to produce less absorbing species. During the laser flash, the absorption of CdS is decreased at wavelengths shortly below the onset of absorption as discussed above, since there exists a certain stationary electron concentration on the illuminated particles. The bleaching as a function of dose is also shown in Figure 18. The bleaching soon strives toward a limiting value, which was explained by a rapid increase in charge carrier recombination rate at doses where more than one electron is stationarily on a particle. I will refrain from discussing further details but would like to emphasize that photoelectron emission has to be considered in connection with bleaching and other effects, such as fluorescence, to understand the overall process of photolysis. From such considerations the following mechanism for photoelectron emission has been derived. It is assumed that photostationary equilibria exist during the 30-ns laser flash:

$$(CdS)_n \underset{k_1}{\overset{h\nu_1}{\rightleftharpoons}} (CdS)_n(e^- + h^+) \underset{k_2}{\overset{h\nu_2}{\rightleftharpoons}} (CdS)_n(e^- + h^+)_2 \xrightarrow{k_e} (CdS)_n(h^+) + e_{aq}^- \quad (14)$$

Absorption of the first photon yields a particle carrying one excited state ($e^- + h^+$). This excited particle may relax to the ground state or absorb a second photon to receive a second excitonic state. The doubly excited particle in turn may lose its second excitation or emit an electron. The specific rate of the second recombination, k_2, is much greater than that of the first recombination, k_1, and that of emission, k_e. The interaction of the two excited states leading to emission can be regarded as an Auger recombination, the annihilation energy of a recombining charge carrier pair being transferred to the electron of the other pair.

G. Charge Carrier Interactions

In the above photoelectron emission experiments, the interaction of two electron–hole pairs produced by the absorption of two photons in a colloidal particle were described. An important question in the discussion of charge carrier interactions in small particles is the actual state of these carriers. First, I would like to draw attention to the fact that the local concentration of the charge carriers is extremely high. For example, when two electron–hole pairs are formed in a 5-nm particle, the local concentration is 2 mol/L.

Immediately after photon absorption the electron and hole are strongly delocalized in the colloidal particle. After time t_1 the electron will be localized in a shallow trap and, similarly, the hole will be trapped after time τ_1 trapping probably occurring on the surface of the particle. The two photons that produce electron emission are not absorbed simultaneously. If the time

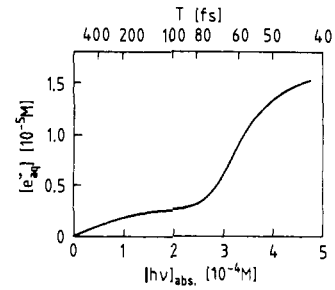

Figure 19. Photoelectron emission from CdS particles at various intensities of a 100-ps laser flash.

T between two successive photon absorptions is longer than t_1, the first electron generated has already relaxed when the second photon arrives; i.e., one is dealing with the interaction of a delocalized electron–hole pair with a relaxed electron. On the other hand, if $T < t_1$, the interaction between two delocalized pairs of charge carriers takes place. With increasing intensity of the laser flash one can expect to move from the first to the second situation. It is clear from these arguments that knowledge of time t_1 is of great importance to understand the effects that are brought about by charge carrier interactions.

Arguments have recently been given for t_1 being extremely short, i.e., far below a pisecond.[7b] The lifetime of band gap fluorescence of CdS particles, in which the surface states are chemically blocked, lies in the 10-ns range.[8c] However, this observation does not contradict the conclusion about t_1 being very much shorter. The localized state of the electron may rapidly return into the delocalized one, i.e., the final fluorescence transition over the band gap occurs out of an equilibrium between the localized and delocalized state of the electron. As the equilibrium lies more on the side of the localized state, the observed lifetime of fluorescence of the delocalized state is longer than its lifetime with respect to localization.

A 100-ps laser flash experiment has recently been carried out by H. Weller in the author's laboratory, the results of which are also understood in terms of t_1 being very short. The laser beam was focused on the colloidal CdS solution and the concentration of emitted electrons measured immediately after the flash. Figure 19 shows the concentration of emitted electrons as a function of the absorbed photon concentration. On the upper abscissa scale the time T between two succeeding photon absorptions in a colloidal particle can be seen. There are two ranges below and above 2.7×10^{-4} M absorbed photons or above and below $T = 80$ fs, respectively. In the lower dose range, the emitted electron concentration increases rather slowly with absorbed dose. This is the range that was previously studied by using a nanosecond laser flash (Figure 17). However, in the high-dose range in Figure 19, the electron yield increases substantially faster with dose. The explanation is that above $T = 80$ fs the condition $T > t_1$ is essentially fulfilled; i.e., one is dealing with the interaction between a delocalized and a localized e^-–h^+ state. Below $T = 80$ fs, interaction between two delocalized states occurs to an increasing extent with increasing dose, and this interaction leads to photoelectron emission with a greater yield. The above mechanism also predicts that the time needed for electron emission itself must be extremely short, i.e., comparable to the time t_1. First

observations with the cocolloid $Zn_{9.5}Cd_{0.05}S$ exposed to a 240-fs laser flash showed that the electrons were indeed emitted during the flash.[43] Under these extremely high intensity conditions, a quantum yield of 0.35 emitted electrons per photon absorbed was observed.

Certain charge carrier interactions have been studied in a fluorescence quenching experiment:[44] A CdS solution was illuminated and the red fluorescence light recorded at right angles. A high-energy electron pulse was then shot into the solution, which practically instantaneously produced hydroxyl radicals. These radicals diffused after the pulse to the colloidal particles and injected a positive hole onto them. It was found that the fluorescence intensity strongly decreased during this reaction. This experiment showed that the fluorescence of a small CdS particle carrying just one excess hole no longer occurs when a photon is absorbed. The mechanism of quenching is not yet fully understood. In the paper cited it was proposed that the red fluorescence of CdS particles is not due to direct trapped electron–hole recombination but is produced when the electron falls from its trap into a deeper one. The direct e^-–h^+ recombination would occur radiationless. However, one can conceive of another mechanism:[31] the annihilation energy of recombination of an e^-–h^+ pair could be used to promote the second hole present to a state of higher energy in the valence band, from where it subsequently is thermalized. Further experiments are needed to understand these phenomena.

H. Conclusions

Certain topics in the field of research on very small semiconductor particles have been selected in the present article to show that many effects occur in this neglected size dimension which were not anticipated even a few years ago. An increasing number of laboratories are now working in this field. This article is written at a time of new developments and therefore in part contains provisory theories and experiments. Modern laser techniques and electronics allow us to carry out very sophisticated experiments on small semiconductor particles but, at the same time, progress also strongly depends on chemical intuition and the development of more refined preparative and analytical methods in subcolloid chemistry.

References

(1) (a) Schmidt, G.; Giebel, U.; Huster, W.; Schwenk, A. *Inorg. Chim. Acta* **1981**, *85*, 97. (b) Kolb, D. M.; Forstmann, F. In *Matrix Isolation Spectroscopy*; Barnes, A. J., Orville-Thomas, W. J., Müller, A., Gaufres, R., Eds.; Reidel: Dordrecht, 1981; p 347. (c) Kolb, D. M. *Ibid.*, p 447. (d) Bennemann, K. H.; Koutecky, J., Eds. *Small Particles and Inorganic Clusters*; North-Holland: Amsterdam, 1985; Parts 1 and 2. (e) Träger, F.; zu Putlitz, G., Eds.; *Metal Clusters*; Springer-Verlag: Berlin, 1986. (f) Morse, M. D. *Chem. Rev.* **1986**, *86*, 1049. (g) Castleman, A. W.; Keesee, R. G. *Annu. Rev. Phys. Chem.* **1986**, *37*, 525. (h) Jena, P.; Rao, B. K.; Khanna, S. N., Eds.; *Physics and Chemistry of Small Clusters*; Plenum Press: New York, 1986.

(2) Birringer, R.; Gleiter, H. *Encyclopedia of Material Science and Engineering*; Cahn, R. W., Ed.; Pergamon Press: New York, 1988; Vol. 1, p 339.

(3) (a) Henglein, A. In *Photochemical Conversion and Storage of Solar Energy*; Rabani, J., Ed.; Weizmann Science Press: Jerusalem, Israel, 1982; Part A, p 115. (b) Henglein, A. *Pure Appl. Chem.* **1984**, *56*, 1215. (c) Henglein, A. In *Modern Trends of Colloid Science in Chemistry and Biology*; Eicke, H.-F., Ed.; Birkhäuser: Basel, 1985; p 126. (d) Henglein, A. *Top. Curr. Chem.* **1988**, *143*, 113. (e) Grätzel, M. *Energy Resources through Photochemistry and Catalysis*; Academic Press: New York, 1983. (f) Kalyanasundaram, K.; Grätzel, M. In *Chemistry and Physics of Solid Surfaces V*; Vanselow, R., Howe, R., Eds.; Springer-Verlag: Berlin, 1984.

(4) (a) Bard, A. J. *Science* **1980**, *207*, 4427. (b) Bard, A. J. *Ber. Bunsen-Ges. Phys. Chem.* **1988**, *92*, 1194.

(5) (a) Alfassi, Z.; Bahnemann, D.; Henglein, A. *J. Phys. Chem.* **1982**, *86*, 4656. (b) Haase, M.; Weller, H.; Henglein, A. *J. Phys. Chem.* **1988**, *92*, 4706. (c) Haase, M.; Weller, H.; Henglein, A. *Ber. Bunsen-Ges. Phys. Chem.* **1988**, *92*, 1103.

(6) Henglein, A.; Kumar, A.; Janata, E.; Weller, H. *Chem. Phys. Lett.* **1986**, *132*, 133.

(7) (a) Wang, Y.; Mahler, W. *Opt. Commun.* **1987**, *61*, 233. (b) Hilinski, E. F.; Lucas, P. A.; Wang, Y. *J. Chem. Phys.* **1988**, *89*, 3435.

(8) (a) Weller, H.; Koch, U.; Gutiérrez, M.; Henglein, A. *Ber. Bunsen-Ges. Phys. Chem.* **1984**, *88*, 649. (b) Dannhauser, T.; O'Neil, M.; Johansson, K.; Whitten, D.; McLendon, G. *J. Phys. Chem.* **1986**, *90*, 6074. (c) Spanhel, L.; Haase, M.; Weller, H.; Henglein, A. *J. Am. Chem. Soc.* **1987**, *106*, 5649.

(9) (a) Spanhel, L.; Weller, H.; Henglein, A. *J. Am. Chem. Soc.* **1987**, *109*, 6632. (b) Spanhel, L.; Henglein, A.; Weller, H. *Ber. Bunsen-Ges. Phys. Chem.* **1987**, *91*, 1359.

(10) (a) Chestnoy, N.; Harris, T. D.; Hull, R.; Brus, L. E. *J. Phys. Chem.* **1986**, *90*, 3393. (b) Alivisatos, A. P.; Harris, A. L.; Levinos, N. J.; Steigerwald, M. L.; Brus, L. E. *J. Chem. Phys.* **1988**, *89*, 4001.

(11) Alivisatos, A. P.; Harris, T. D.; Brus, L. E.; Jayaraman, A. *J. Chem. Phys.* **1988**, *89*, 5979.

(12) Thayer, A. M.; Steigerwald, M. L.; Duncan, T. M.; Douglas, D. C. *Phys. Rev. Lett.* **1988**, *60*, 2675.

(13) Henglein, A.; Lilie, J. *J. Am. Chem. Soc.* **1981**, *103*, 1059.

(14) Henglein, A. *Ber. Bunsen-Ges. Phys. Chem.* **1980**, *84*, 253.

(15) Henglein, A.; Tausch-Treml, R. *J. Colloid Interface Sci.* **1981**, *80*, 84.

(16) (a) Henglein, A. *Ber. Bunsen-Ges. Phys. Chem.* **1977**, *81*, 556. (b) Henglein, A. *Elektrochemie* der Metalle *DECHEMA Monogr.* **1983**, *93*, 163.

(17) Mostafavi, M.; Marignier, J. L.; Amblard, J.; Belloni, J. *Radiat. Phys. Chem.* **1989**, *34*, 605.

(18) Mosseri, S.; Henglein, A.; Janata, E. *J. Phys. Chem.* **1989**, *93*, 6791.

(19) Gingerich, K. A.; Cocke, D. L.; Miller, F. *J. Chem. Phys.* **1976**, *64*, 4027.

(20) Breitenkamp, M.; Henglein, A.; Lilie, J. *Ber. Bunsen-Ges. Phys. Chem.* **1976**, *80*, 973.

(21) Tausch-Treml, R.; Henglein, A.; Lilie, J. *Ber. Bunsen-Ges. Phys. Chem.* **1978**, *82*, 1335.

(22) Henglein, A. *Chem. Phys. Lett.* **1989**, *154*, 473.

(23) Weller, H.; Fojtik, A.; Henglein, A. *Chem. Phys. Lett.* **1985**, *117*, 485.

(24) Henglein, A.; Fojtik, A.; Weller, H. *Ber. Bunsen-Ges. Phys. Chem.* **1987**, *91*, 441.

(25) (a) Brus, L. E. *J. Chem. Phys.* **1983**, *79*, 5566. (b) Brus, L. E. *J. Chem. Phys.* **1984**, *80*, 4403. (c) Brus, L. E. *J. Phys. Chem.* **1986**, *90*, 2555. (d) Brus, L. E. *IEEE J. Quantum Electron.* **1986**, *QE-22*, 1909.

(26) Schmidt, H. M.; Weller, H. *Chem. Phys. Lett.* **1986**, *129*, 615.

(27) Weller, H.; Schmidt, H. M.; Koch, U.; Fojtik, A.; Baral, S.; Henglein, A.; Kunath, W.; Weiss, K.; Dieman, E. *Chem. Phys. Lett.* **1986**, *124*, 557.

(28) Wang, Y.; Suna, A.; Mahler, W.; Kasowski, R. *J. Chem. Phys.* **1987**, *87*, 7315.

(29) Peterson, M. W.; Nenadovic, M. T.; Rajh, T.; Herak, R.; Micic, O. I.; Goral, J. P.; Nozik, A. J. *J. Phys. Chem.* **1988**, *92*, 1400.

(30) Gutiérrez, M.; Henglein, A. *Ultrasonics* **1989**, *27*, 259.

(31) Gallardo, S.; Gutiérrez, M.; Henglein, A. *Ber. Bunsen-Ges. Phys. Chem.* **1989**, *93*, 1080.

(32) (a) Fischer, Ch.-H.; Lilie, J.; Weller, H.; Katsikas, L.; Henglein, A. *Ber. Bunsen-Ges. Phys. Chem.* **1989**, *93*, 61. (b) Fischer, Ch.-H.; Weller, H.; Katsikas, L.; Henglein, A. *Langmuir* **1989**, *5*, 429.

(33) Steigerwald, M. L.; Alivisatos, A. P.; Gibson, J. M.; Harris, T. D.; Kortan, R.; Muller, A. J.; Thayer, A. M.; Duncan, T. M.; Douglas, D. C.; Brus, L. E. *J. Am. Chem. Soc.* **1988**, *110*, 3046.

(34) (a) Nosaka, Y.; Yamaguchi, K.; Miyama, H.; Hayashi, H. *Chem. Lett.* **1988**, 605. (b) Fischer, Ch.-H.; Henglein, A. *J. Phys. Chem.* **1989**, *93*, 5578.

(35) Hayes, D.; Micic, O. I.; Nenadovic, M. T.; Swayambunathan, V.; Meisel, D. *J. Phys. Chem.* **1989**, *93*, 4603.

(36) Spanhel, L.; Weller, H.; Fojtik, A.; Henglein, A. *Ber. Bunsen-Ges. Phys. Chem.* **1987**, *91*, 88.

(37) Henglein, A.; Gutiérrez, M.; Weller, H.; Fojtik, A.; Jirkovský, J. *Ber. Bunsen-Ges. Phys. Chem.* **1989**, *93*, 593.

(38) (a) Burstein, E. *Phys. Rev.* **1954**, *93*, 632. (b) Moss, T. S. *Proc. Phys. Soc., London* **1954**, *76*, 775.

(39) Liu, C.; Bard, A. J. *J. Phys. Chem.* **1989**, *93*, 3232.

(40) Kormann, C.; Bahnemann, D. W.; Hoffman, M. R. *J. Phys. Chem.* **1988**, *92*, 5196.

(41) Haase, M.; Weller, H.; Henglein, A. *J. Phys. Chem.* 1988, *92*, 482.
(42) Gurevich, Yu. Ya.; Pleskov, Yu. V.; Rotenberg, Z. A. *Photoelectrochemistry*; Consultants Bureau: New York, 1980.
(43) Ernsting, N. P.; Kaschke, M.; Weller, H.; Katsikas, L. *J. Opt. Soc. Am. B.*, in press.
(44) Kumar, A.; Janata, E.; Henglein, A. *J. Phys. Chem.* 1988, *92*, 2587.